CONTRAST-BASED REGISTRATION OF LEFT ATRIA TO FLUOROSCOPIC IMAGE SEQUENCES BY TEMPORAL MARKOW FILTERING AND MOTION REGULARIZATION

M. Hoffmann[⋆]*, N. Strobel*[‡]*, J. Hornegger*[⋆◦]*, A. Maier*[⋆◦]

[⋆] Pattern Recognition Lab, Friedrich-Alexander-Universität Erlangen-Nürnberg, Erlangen, Germany
[‡] Siemens Healthcare GmbH, Forchheim, Germany
[◦] Erlangen Graduate School in Advanced Optical Technologies (SAOT)

ABSTRACT

Atrial fibrillation is a common heart arrhythmia which can be treated minimally invasively using catheters. Navigation during the procedure can be performed under fluoroscopic guidance. To overcome the low soft tissue contrast of fluoroscopic images, they can be fused with a pre-interventionally acquired 3-D segmentation of the patient's left atrium (LA). As catheter positioning is crucial to destroy arrhythmogenic tissue of the LA, better navigation by fusing the 3-D LA shape with fluoroscopic images is important. Furthermore, additional graphical information can be visualized together with the LA once the LA segmentation has been registered to the fluoroscopic images. Registration can be performed based on contrast agent which is injected into the LA and then captured as part of an X-ray sequence. Recent publications have shown that an intensity-based registration using the contrasted area leads to good results. However, the dependency between the frames of an X-ray image sequence has not been exploited yet. Since contrast agent is injected over a certain period of time and captured over many frames, we propose a time-dependent registration. To this end, we introduce motion regularization to ensure small motion of the overlay between successive frames. We propose two methods for motion regularization. One method is based on a Markov chain model of the heart motion, the other approach introduces a motion regularizer into the similarity measure used for registration. The Markov chain approach reduces the registration error significantly from 7.9 ± 6.3 mm to 5.7 ± 4.6 mm. The motion regularizer also reduces the registration error significantly, but less than the Markov approach.

Index Terms— Registration, Electrophysiology

1. INTRODUCTION

Atrial fibrillation is a wide-spread arrhythmia of the left atrium (LA) and is a leading cause of stroke [1]. One treatment option is catheter ablation which is performed minimally invasively using either radiofrequency catheters or so called single-shot devices, e.g., the cryoballoon [2]. The catheters are guided over the right atrium into the LA via a transseptal puncture. Guidance during treatment can be accomplished using electro-anatomical mapping systems or fluoroscopy involving C-arm X-ray systems. One drawback of fluoroscopic guidance is the lack of 3-D anatomical information. To overcome this problem, a 3-D heart model of the patient can be obtained either pre-operatively or intra-operatively, e.g., using CT, MRI or C-arm CT followed by a segmentation step. This model can then be overlaid on fluoroscopic images to provide 3-D anatomical information [3].

To display a properly aligned overlay image, the coordinate system of the 3-D model needs to be registered to the 2-D images obtained with the C-arm X-ray system. Registration can be performed manually when the shape of the left atrium is enhanced by injecting contrast agent [4]. Contrast injection can be used at the beginning of the procedure to verify puncture success and the sheath position within the LA [5]. Using a biplane C-arm system, image sequences from two views, A and B with an angular offset of, e.g., 90 degrees, can be acquired together. By registering the LA model to the angiographic sequences of both views simultaneously, a 3-D/2-D registration can be performed [6, 4], see Figure 1.

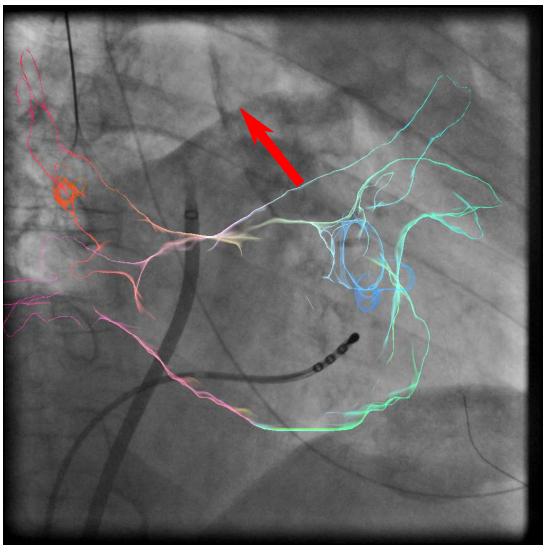

Fig. 1. Registration of a 3-D model segmented from a preoperative MRI scan to fluoroscopic images. This can be accomplished by aligning the 3-D model to anatomical structures of the LA highlighted by contrast agent. This implies moving the model along the red arrow in this case.

An automatic contrast-based registration has been proposed by Thivierge-Gaulin *et al.* [7]. Here, a transform of the LA model is found such that the image intensities within the projected shadow of the left atrium as well as the intensities outside the projected shadow are homogeneous. A different approach by Zhao *et al.* [8] computes digitally rendered radiographies of a CT volume showing the LA and optimizes the transformation using gradient correlation. To keep the contrast burden to the patient low, often only a small amount of contrast agent is injected into the LA such that it is only partially visible in the X-ray images. In these cases, an automatic contrast-based registration is more challenging. This problem was addressed by a

recent method that matches edges of the 3-D LA model to edges in the angiography while enforcing a consistency condition for the contrast agent distribution [9]. A different approach using a segmentation of the coronary sinus (CS) catheter in the CT- or MRI-volume and a reconstruction of the CS catheter from two X-ray images was proposed by Brost *et al.* [10].

All these approaches have in common that the frames of an angiographic sequence are treated independently. However, if the LA motion is captured using a sufficiently high frame rate, valuable information can be obtained by taking motion into account. This can be accomplished by enforcing a motion constraint on the position of the LA model in 3-D. We propose, based on the work in [9], a registration for all contrasted frames of an angiography series that introduces dependencies between single frames within a sequence to end up with more robust registration results. We investigate two different approaches: The first approach applies a retrospective motion constraint to refine already computed registration results using a confidence-based temporal filtering method implemented as a Markov process. The second approach introduces a regularizer on the position of the left atrium to improve registration by constraining the estimated LA motion.

2. REGISTRATION

In this section, we summarize briefly the registration of a single frame which is described in detail in [9]. The main idea of the registration is to compare images showing the contrast agent and its edges to corresponding images rendered from the 3-D model. The comparison is performed using an intensity-based similarity measure.

For each frame $\boldsymbol{I}_\mathrm{c}$ of the angiography containing contrast agent, a difference image is computed using an uncontrasted frame $\boldsymbol{I}_\mathrm{u}$, $\boldsymbol{I}_{DSA} = \boldsymbol{I}_\mathrm{u} - \boldsymbol{I}_\mathrm{c}$. Based on this image, a binary image $\boldsymbol{I}_\mathrm{thr}$ of the contrast agent is obtained using a threshold. In the next step, an image $\boldsymbol{I}_\mathrm{DOG}$ showing edges of the contrast agent is calculated by applying a derivative of Gaussian (DOG). For a given transformation T, 2-D feature images are rendered from the 3-D model for both views A and B: The first pair of feature images, $\boldsymbol{S}_T^\mathrm{A}$ and $\boldsymbol{S}_T^\mathrm{B}$ show the projected shadow of the LA model. The second pair, $\boldsymbol{E}_T^\mathrm{A}$ and $\boldsymbol{E}_T^\mathrm{B}$ show edges of the 3-D model as they appear from the respective viewing direction. From the normalized cross correlation

$$\rho_\mathrm{n}(\boldsymbol{I}_1, \boldsymbol{I}_2) = \sum_{x=0}^{n}\sum_{y=0}^{m} \frac{(\boldsymbol{I}_1(x,y) - \mu_1)\cdot(\boldsymbol{I}_2(x,y) - \mu_2)}{\sigma_1 \cdot \sigma_2}, \quad (1)$$

similarity measures are derived as

$$\rho_\mathrm{shad}^\mathrm{DSA}(T) = \rho_\mathrm{n}(\boldsymbol{I}_{DSA}^\mathrm{A}, \boldsymbol{S}_T^\mathrm{A}) \cdot \rho_\mathrm{n}(\boldsymbol{I}_{DSA}^\mathrm{B}, \boldsymbol{S}_T^\mathrm{B}), \quad (2)$$

$$\rho_\mathrm{shad}^\mathrm{thr}(T) = \rho_\mathrm{n}(\boldsymbol{I}_\mathrm{thr}^\mathrm{A}, \boldsymbol{S}_T^\mathrm{A}) \cdot \rho_\mathrm{n}(\boldsymbol{I}_\mathrm{thr}^\mathrm{B}, \boldsymbol{S}_T^\mathrm{B}), \quad (3)$$

$$\rho_\mathrm{edge}(T) = \rho_\mathrm{n}(\boldsymbol{I}_\mathrm{DOG}^\mathrm{A}, \boldsymbol{E}_T^\mathrm{A}) \cdot \rho_\mathrm{n}(\boldsymbol{I}_\mathrm{DOG}^\mathrm{B}, \boldsymbol{E}_T^\mathrm{B}). \quad (4)$$

For the third similarity measure, a contrast agent distribution estimate (CADE) $C_T^\text{3-D}(\boldsymbol{v})$ is computed. The 3-D model is represented as a binary volume and a voxel $\boldsymbol{v}$ is considered as contrasted if (a) it is located within the LA, and (b) its projection onto both imaging planes after applying the transformation T hits a contrasted pixel. All contrasted voxels are forward projected into 2-D finally yielding two binary images $\boldsymbol{C}_T^\mathrm{A}$, $\boldsymbol{C}_T^\mathrm{B}$. The CADE-based similarity measure is then defined as

$$\rho_\mathrm{CADE}(\boldsymbol{I}_\mathrm{thr}^\mathrm{A}, \boldsymbol{I}_\mathrm{thr}^\mathrm{B}, T) = \rho_\mathrm{n}(\boldsymbol{I}_\mathrm{thr}^\mathrm{A}, \boldsymbol{C}_T^\mathrm{A}) \cdot \rho_\mathrm{n}(\boldsymbol{I}_\mathrm{thr}^\mathrm{B}, \boldsymbol{C}_T^\mathrm{B}). \quad (5)$$

In practice, the transformation T can be implemented as a pure 3-D translation. The rotation is neglectable as the patient are positioned similarly during the 3-D scan and during the intervention itself [10, 6, 9]. Therefore, we use as transformation T a translation vector. We consider our 3-D model to be mean-centered, i.e., the center of mass is located at the origin of the coordinate system. As a consequence, the position $\boldsymbol{x}$ of the model, i.e., the center of mass is identical to the translation vector T and we will use both interchangeably.

3. MOTION CONSTRAINED REGISTRATION

3.1. Confidence-Based Temporal Markov Filtering

In our first approach for motion compensated registration, we model the position of the LA model in 3-D as a time-dependent continuous Markov chain of first order. The states are positions of the model in $\mathbb{R}^3$, $\boldsymbol{\chi}_i$ denotes the actual position of the LA in the i-th contrasted frame, $\boldsymbol{x}_i$ denotes the estimate of the position for the i-th frame. The probability, that at time point i the position $\boldsymbol{x}_i$ is observed is denoted as $P(\boldsymbol{\chi}_i = \boldsymbol{x}_i)$ or, for convenience, simply as $P(\boldsymbol{x}_i)$. The transition probability from one state into another does not depend on frame number and is denoted as $P(\boldsymbol{x}_i \to \boldsymbol{x}_{i+1})$.

Transition probabilities and state probabilities have different functions: The transition probabilities govern how LA positions, as estimated for the previous and the successive frame, are averaged. They are highest if the overlay does not move. The state probability controls how much averaging is performed for a single frame, i.e., how much it is moved away from its current position. We will base the state probability on a confidence measure that reflects the estimated accuracy associated with a computed registration result for a frame. For frames with a high-confidence registration result, the transition probability has only little influence and little averaging is performed. More averaging is applied to frames where the computed registration result is less certain.

At the end, a sequence of positions $\boldsymbol{x}_1, \ldots, \boldsymbol{x}_n$ is to be determined such that the term

$$P(\boldsymbol{x}_1, \ldots, \boldsymbol{x}_n) = P(\boldsymbol{x}_1) \cdot \prod_{t=2}^{n} \left(P(\boldsymbol{x}_{t-1} \to \boldsymbol{x}_t) \cdot P(\boldsymbol{x}_t)\right) \quad (6)$$

is maximized. The state probabilities and the transition probability are determined as follows.

3.1.1. State Probability

The probability of the LA for being at position $\boldsymbol{x}_i$ at frame i is directly related to the contrast agent in frame i. The most probable position $\boldsymbol{x}_i'$, ignoring the dependency on other frames, is defined by the registration result for this single frame. This registration result is obtained by maximizing one of the similarity measures ρ defined in Eqs. (2) - (4) or a combination of them.

As the similarity measure depends on the image content, we denote the similarity measure for frame i by ρ_i. Zhao *et al.* [8] suggested to use the value $\rho_i(\boldsymbol{x}_i')$ as a confidence measure. That is, to select from all N registration results the frame i where $\rho_i(\boldsymbol{x}_i')$ is maximum and use this as registration result for the whole procedure. We confirmed that $\rho_i(\boldsymbol{x}_i)$ is indeed correlated with the registration error and can therefore be used as a confidence measure. Next, we define a function $e(\rho_i(\boldsymbol{x}_i))$ which provides us with an error estimate based on the value of ρ_i. This function is obtained in a training step using linear regression. Using the position $\boldsymbol{x}_i'$ of the LA found during optimization for frame i, the probability $P(\boldsymbol{x}_i)$ can be modelled as normal distribution

$$P(\boldsymbol{x}_i) = \mathcal{N}\left(\boldsymbol{x}_i; \boldsymbol{x}_i', \boldsymbol{\Sigma}_i\right). \quad (7)$$

Table 1. Translation errors

All frames			
Objective function	No motion constraint	Markov filtering	Motion regularizer
$\rho_{\text{shad}}^{\text{DSA}} + \rho_{\text{edge}}$	8.9±6.1 mm	6.9±3.9 mm	7.6±4.6 mm
$\rho_{\text{shad}}^{\text{thr}} + \rho_{\text{edge}}$	9.3±7.2 mm	7.0±4.2 mm	8.4±5.0 mm
$\rho_{\text{CADE}} + \rho_{\text{edge}}$	8.3±6.4 mm	6.2±4.3 mm	7.8±5.7 mm
Initial injections			
Objective function	No motion constraint	Markov filtering	Motion regularizer
$\rho_{\text{shad}}^{\text{DSA}} + \rho_{\text{edge}}$	8.3±6.6 mm	6.5±4.3 mm	7.5±5.1 mm
$\rho_{\text{shad}}^{\text{thr}} + \rho_{\text{edge}}$	8.3±6.7 mm	6.1±4.4 mm	7.3±4.6 mm
$\rho_{\text{CADE}} + \rho_{\text{edge}}$	7.9±6.3 mm	5.7±4.6 mm	6.3±4.8 mm
Clinical experts	3.3±2.7 mm		

By setting the covariance matrix $\mathbf{\Sigma}_i$ to $\mathbf{1} \cdot e(\rho_i(\boldsymbol{x}_i'))$, we incorporate our confidence range.

3.1.2. Transition Probability

The transition probability $P(\boldsymbol{x}_{t-1} \rightarrow \boldsymbol{x}_t)$ states how likely a movement of the LA is from frame $t-1$ to t. As frame rates may differ, the frame rate r of the sequence needs to be taken into account. The position of the LA observed over multiple breathing cycles moves about a mean position. So, the mean motion can be set to 0. Based on annotated training data, we computed for each frame i the velocity $\boldsymbol{v}_i = (\boldsymbol{x}_t - \boldsymbol{x}_{t-1}) \cdot r$ and the covariance matrix $\mathbf{\Sigma}_{\boldsymbol{v}}$ of the velocities. This gives us an estimate for how probable a motion is. The probability of a transition $\boldsymbol{x}_{t-1} \rightarrow \boldsymbol{x}_t$ is then modelled as a normal distribution

$$P(\boldsymbol{x}_{t-1} \rightarrow \boldsymbol{x}_t) = \mathcal{N}\left((\boldsymbol{x}_t - \boldsymbol{x}_{t-1}) \cdot r; 0, \mathbf{\Sigma}_{\boldsymbol{v}}\right). \tag{8}$$

3.1.3. Most Probable State Sequence

The most likely state sequence is defined by

$$\boldsymbol{x}_1^*, \ldots, \boldsymbol{x}_n^* = \underset{\boldsymbol{x}_i, \ldots, \boldsymbol{x}_n}{\operatorname{argmax}} P(\boldsymbol{x}_i, \ldots, \boldsymbol{x}_n). \tag{9}$$

Optimization is done using a log-likelihood method: By applying the logarithm to Eq. 6, we get

$$\begin{aligned} \boldsymbol{x}_1^*, \ldots, \boldsymbol{x}_n^* = \underset{\boldsymbol{x}_1 \ldots \boldsymbol{x}_n}{\operatorname{argmax}} -\frac{1}{2} \Bigg(& (\boldsymbol{x}_1 - \boldsymbol{x}_1')^T \mathbf{\Sigma}_1^{-1} (\boldsymbol{x}_1 - \boldsymbol{x}_1') \\ & + \sum_{i=2}^{n} \Big((\boldsymbol{x}_i - \boldsymbol{x}_i')^T \mathbf{\Sigma}_i^{-1} (\boldsymbol{x}_i - \boldsymbol{x}_i') \; + \\ & r \cdot (\boldsymbol{x}_i - \boldsymbol{x}_{i-1})^T \mathbf{\Sigma}_{\boldsymbol{v}}^{-1} (\boldsymbol{x}_i - \boldsymbol{x}_{i-1}) \cdot r \Big) \Bigg) \end{aligned} \tag{10}$$

which is a convex optimization problem that can be solved using the (L)BFGS method [11].

3.2. Motion Regularization

In the Markov filtering approach, the uncertainty of the registration result is introduced afterwards in Eq. 7 by the covariance matrix $\mathbf{\Sigma}_i$ which incorporates the confidence range of the solution for frame i. This uncertainty measure is decoupled from the registration of the frames but is computed explicitly based on previous observations of the registration error. However, uncertainty is also represented implicitly in the shape of the objective function around the global optimum. For example, the shape might be rather plateau-like when having a high uncertainty.

Therefore, we propose to add a regularizer to the optimization function which alters the shape of the objective function in order to favor small motion between successive frames, similar to an approach by Berger *et al.* [12]. So, instead of optimizing the objective function ρ for each frame independently, a joint optimization

$$\boldsymbol{x}_1^*, \ldots, \boldsymbol{x}_n^* = \underset{\boldsymbol{x}_1 \ldots \boldsymbol{x}_n}{\operatorname{argmax}} \sum_{i=1}^{n} \rho(\boldsymbol{x}_i) - \alpha \sum_{i=1}^{n-1} ||\boldsymbol{x}_{i+1} - \boldsymbol{x}_i||_2. \tag{11}$$

for all frames is performed.

As the objective space is rather complex and contains several local optima, an initialization needs to be found that is close to the optimal solution. In our case, the $\boldsymbol{x}_i$ are initialized by performing an independent registration for each single frame i. Then, Eq. 11 is optimized by a LBFGS optimizer using approximated gradients.

4. EXPERIMENTS AND RESULTS

For evaluation of our method, we used the same data as in [9]. This data set comprised 21 clinical biplane angiography sequences from 10 different patients. For all 133 frames, a ground-truth-annotation from two or more physicians was available. The data can be split into 11 sequences showing an initial contrast injection at the beginning of the procedure and 10 sequences showing a subsequent injection. Typically, for initial injections, more contrast agent is used such that the LA is outlined better.

The training of the error estimate function $e(\rho_i(\boldsymbol{x}_i))$ and the transition probability covariance matrix $\Sigma_{\boldsymbol{v}}$ as well as the determination of a suited regularizer weight α was performed in a leave-one-patient-out cross-validation. In our experiments, we first did a per-frame-registration as described in [9] and performed then our proposed motion compensations. The results are listed in Table 1. The mean error for a Markov filtering on the results achieved using the CADE similarity measure was 6.2±4.3 mm for all sequences and 5.7±4.6 mm when only initial injections were considered. The respective median errors were 4.7 mm and 4.0 mm. A Wilcoxon signed rank test [13] showed that the results obtained by the Markov filtering were in all cases significantly better than the results from the regularizer-based approach.

The overall computation time is made up of the computation of the initial registration which takes between 13 and 27 seconds [9] per frame and the subsequent motion filtering operation. Experiments

were run on a PC having an Intel i7, 2.6 GHz CPU and a NVidia K1000M GPU. The runtime of the Markov filtering is 173 ± 124 ms per sequence, the optimization of the function using the regularizer takes 6.8 ± 5.6 minutes if $\rho_{\mathrm{CADE}}+\rho_{\mathrm{edge}}$ is used as objective function and 1.3 ± 1.0 minutes for the other objective functions.

5. DISCUSSION AND CONCLUSIONS

In our experiments, the Markov filtering outperformed the motion regularizer based approach. This result confirms that the value of the similarity measure is a good measure for uncertainty. The best results were achieved using the CADE measure, which has also been shown in [9] to outperform other similarity measures. In our new results, the mean error was close to the clinical relevant threshold of 5.0 mm [14], while the median error was below this threshold.

Actually, the transition probability depends not only on the frame rate r but also on the current breathing phase. Cardiac motion is negligible compared to breathing motion as it rather deforms the LA. In future work, if the breathing phase can be estimated [15], motion in superior direction should have, e.g., a higher probability during the inhale phase. During exhale phase, motion in inferior direction should be considered as more likely. This could be achieved, e.g., by estimating the mean value and the covariance matrix separately for different stages of the breathing cycle.

The runtime of the simple regularizer-based approach is relatively high. This is because the similarity measure needs to be computed in each iteration for all frames. A speedup can, however, be easily achieved by using different hardware. For example, using the same GPU as in [9] would result in a speedup factor of approx. 3, a more recent GPU will probably reduce computation time even more.

An analysis showed that the regularizer-based method is sensitive to the selection of α. To find a theoretical lower bound, for each case, α was not determined in a leave-one-out training step but chosen optimally. In this case, almost the same results as for the Markov approach could be achieved. As a single value of α does not generalize to all images, further effort would be needed to find a method with which to determine a good α-value for unknown images. However, the accuracy which is theoretically achievable by an optimal selection of α can also be achieved with less runtime using the Markov-approach. So there is practically no need for finding a method for the selection of α.

Regardless of the filtering method, results improved in both cases significantly compared to an unfiltered registration. This shows that motion filtering is essential to obtain reliable registration results. In a future work, a similar approach could be also applied to device based registration [10].

Compared to selecting the frame with the highest confidence for registration as proposed by [8], our filtering approach allows the physician to choose the frame, as good results are obtained for all frames. This has the advantage that the physician is free to choose a frame, e.g., depending on the breathing phase or heart phase.

Acknowledgments and Disclaimer. This work was supported by Siemens Healthcare GmbH. The concepts and information presented in this paper are based on research and are not commercially available.

6. REFERENCES

[1] P.A. Wolf, R.D. Abbott, and W.B. Kannel, "Atrial fibrillation as an independent risk factor for stroke: the Framingham study," *Stroke*, vol. 22, no. 8, pp. 983–988, 1991.

[2] V. Fuster, L. Rydén, D. Cannom, H. Crijns, et al., "ACC/AHA/ESC 2006 Guidelines for the Management of Patients With Atrial Fibrillation - Executive Summary," *Journal of the American College of Cardiology*, vol. 48, no. 4, pp. 854, 2006.

[3] S. De Buck, F. Maes, J. Ector, J. Bogaert, et al., "An Augmented Reality System for Patient-Specific Guidance of Cardiac Catheter Ablation Procedures," *Medical Imaging, IEEE Transactions on*, vol. 24, no. 11, pp. 1512 –1524, nov. 2005.

[4] M. Hoffmann, F. Bourier, N. Strobel, and J. Hornegger, "Structure-Enhancing Visualization for Manual Registration in Fluoroscopy," in *Bildverarbeitung für die Medizin 2013*, Berlin Heidelberg, 2013, Informatik aktuell, pp. 241–246, Springer.

[5] T. Feldman and W. G. Fisher, *Problem Oriented Approaches in Interventional Cardiology*, chapter Transseptal puncture, pp. 203–218, CRC Press, 2007.

[6] F. Bourier, D. Vukajlovic, A. Brost, J. Hornegger, N. Strobel, and K. Kurzidim, "Pulmonary Vein Isolation Supported by MRI-Derived 3D-Augmented Biplane Fluoroscopy: A Feasibility Study and a Quantitative Analysis of the Accuracy of the Technique," *Journal of Cardiovascular Electrophysiology*, vol. 24, no. 2, pp. 113–120, 2013.

[7] D. Thivierge-Gaulin, C.R. Chou, A. Kiraly, C. Chefd'Hotel, N. Strobel, and F. Cheriet, "3d-2d registration based on mesh-derived image bisection," in *Biomedical Image Registration*. 2012, vol. 7359 of *Lecture Notes in Computer Science*, pp. 70–78, Springer Berlin Heidelberg.

[8] X. Zhao, S. Miao, L. Du, and R. Liao, "Robust 2-d/3-d registration of ct volumes with contrast-enhanced x-ray sequences in electro-physiology based on a weighted similarity measure and sequential subspace optimization," in *Acoustics, Speech and Signal Processing (ICASSP), 2013 IEEE International Conference on*, May, 26th - 31st 2013, pp. 934–938.

[9] M. Hoffmann, C. Kowalewski, A. Maier, K. Kurzidim, N. Strobel, and J. Hornegger, "3-D/2-D Registration of Cardiac Structures by 3-D Contrast Agent Distribution Estimation," *arXiv:1601.06062 [cs.CV]*, 2016.

[10] A. Brost, F. Bourier, L. Yatziv, M. Koch, et al., "First steps towards initial registration for electrophysiology procedures," in *Medical Imaging 2011: Visualization, Image-Guided Procedures, and Modeling*. 2011, vol. 7964, p. 79641P, SPIE.

[11] D. Goldfarb, "A family of variable-metric methods derived by variational means," *Mathematics of computation*, vol. 24, no. 109, pp. 23–26, 1970.

[12] M. Berger, K. Müller, J.-H. Choi, A. Aichert, et al., "2D/3D Registration for Motion Compensated Reconstruction in Cone-Beam CT of Knees Under Weight-Bearing Condition," in *IFMBE Proceedings*, D. A. Jaffray, Ed., 2015, pp. 54–57.

[13] F. Wilcoxon, "Individual comparisons by ranking methods," *Biometrics bulletin*, pp. 80–83, 1945.

[14] A.P. King, R. Boubertakh, K.S. Rhode, Y.L. Ma, et al., "A subject-specific technique for respiratory motion correction in image-guided cardiac catheterisation procedures," *Medical Image Analysis*, vol. 13, no. 3, pp. 419 – 431, 2009.

[15] P. Fischer, T. Pohl, and J. Hornegger, "Real-Time Respiratory Signal Extraction from X-Ray Sequences using Incremental Manifold Learning," in *2014 IEEE 11th International Symposium on Biomedical Imaging (ISBI)*, 2014, pp. 915–918.